Some aspects of the Statistical Mechanics of concentrated colloidal suspensions

Thierry Biben, Jean-Pierre Hansen, Hartmut Löwen

Laboratoire de Physique, Ecole Normale Supérieure de Lyon, 69364 Lyon Cedex 07, France

ABSTRACT: The Statistical Mechanics description of concentrated colloidal suspensions is illustrated by a few recent applications which emphasize both the analogies and the differences between mesoscopic suspensions and simple atomic liquids. The aspects which are briefly reviewed in this paper are phase transitions, the kinetic glass transition, density profiles of suspensions under gravity and phase separation in highly asymmetric hard sphere mixtures.

1. INTRODUCTION

The name "colloidal suspensions" covers an extremely wide variety of physico-chemical systems involving "mesoscopic" particles (in the size range $10 \lesssim \sigma \lesssim 10^3$ nm if σ denotes some characteristic diameter) dispersed in a suspending fluid like water or some organic solvent. Restriction will be made in the following to rigid, spherical colloidal particles. The main point of the present lectures will be to show, on the basis of a few examples, that under suitable conditions, concentrated suspensions of such particles exhibit strong analogies with simple liquids, despite the very different size and time scales involved. However these similarities should not conceal some fundamental differences, notably as far as the dynamics are concerned.

Any "first principles" Statistical Mechanics description is necessarily based on a knowledge of the mutual interactions between particles, which are generally simplified in the framework of simple models, chosen so as to capture the essential features of interparticle forces. The two universal characteristics of these interactions are linked to the fact that colloids are made up of $10^6 - 10^{12}$ atoms, depending on their size. Hence Born repulsion between Brownian particles will set in when their mutual distance r approaches their diameter, whereas the Van der Waals interactions between atoms will add up to the familiar attractive Hamaker potential $v_H(r)$, which decays like $1/r^6$ for $r \gg \sigma$, but diverges at contact according to :

$$\lim_{r \to \sigma^+} v_H(r) = -\frac{H\sigma}{24(r-\sigma)} \tag{1}$$

S.-H. Chen et al. (eds.),
Structure and Dynamics of Strongly Interacting Colloids and Supramolecular Aggregates in Solution, 23–37.

where $H \simeq 10^{-20}$ J is Hamaker's constant [1,2]. This singular attraction leads to irreversible flocculation (or coagulation) of the particles, if no special care is taken to stabilize the suspension.

Stabilization may be achieved by "coating" the colloidal particles to prevent them from touching. There are essentially two methods to stabilize the suspension. Steric stabilization is achieved by grafting or adsorbing polymer chains on the surface of the particles; this leads to a repulsion of entropic origin (originating in the reduction of polymer phase space when two particles approach), which may, in first approximation, be modelled by a simple hard sphere interaction. Charge stabilization results when radicals at the surface ionize in a polar suspending fluid (e.g. water), so that the particles carry a surface charge, leading to the formation of a double layer. Linearized Poisson-Boltzmann theory then leads, under appropriate conditions, to a screened Coulomb interaction of the form [1,2]:

$$v(r) = U_0 \frac{a}{r} \exp\left(-\kappa \frac{(r-a)}{a}\right) \qquad (2)$$

where U_0 is determined by the charge Ze carried by the Brownian particles and the dielectric permittivity ϵ of the solvent, a is a suitable length scale (e.g. $a = \sigma$) and $\kappa = a/\lambda$ is the reduced inverse Debye screening length governed by the concentration of the counterions and added salt. The total interaction energy (or rather free energy) is the sum of (2) and $v_H(r)$, resulting in the celebrated DLVO potential [1,2]. Note that the interactions may be largely "tuned" by varying salt concentration, and hence κ. In particular at low concentration (i.e. small κ), the screened Coulomb repulsion "masks" completely the Van der Waals attractions. Similarily the latter may be practically suppressed in sterically stabilized suspensions in organic solvents by "index-matching".

To summarize the previous discussion, provided Van der Waals attractions may be neglected, the two fundamental models, which will be extensively used in the following, are: the hard sphere (HS) model and the screened Coulomb (or Yukawa) model (2). Both are "primitive" models of suspensions in so far as they replace the suspending fluid by a structureless, inert continuum. Solvent effects, such as solvation, Stokesian friction and hydrodynamic interactions are neglected. The two latter are velocity-dependent and hence should not contribute to the static equilibrium properties of the suspension, like the osmotic pressure or the pair structure, but they play of course a fundamental role as far as dynamics are concerned. An example will be discussed in section 3.

The exact status of eqn.(2) to describe the effective interaction in charge-stabilized suspensions has been the object of strong debate. To go beyond the linearized Poisson-Boltzmann approach, one may treat the counter-and salt ions as discrete entities, and use the non-linear integral equations of the theory of liquids [3] to describe the highly asymmetric mixture of polyions and microions [4]. An alternative approach, more similar in spirit to Poisson-Boltzmann theory, but including correlations between microions, is presently being investigated [5]. This approach is a classical Statistical Mechanics version of the powerful ab initio Molecular Dynamics scheme developed by Car and

Parrinello to simulate covalent and metallic systemes [6]. Equations-of-motion are derived from a Lagrangian depending on the discrete positions and velocities of the polyions, while the Fourier components of the macroion charge distribution $\rho(\vec{r})$ are considered as additional dynamical variables which are coupled among themselves and to the polyion positions within a simple density functional formulation. This scheme accounts for the instantaneous fluctuations of $\rho(\vec{r})$ and for the distortions and interpenetration of double layers associated with neigbouring polyions; the resulting effective forces between the latter naturally include more-than-two-body contributions.

A fundamental difference between atomic and colloidal systems is the intrinsic polydispersity of the latter. While atomic "democracy" is imposed by Quantum Mechanics, the complex chemical composition of colloidal particles leads to unavoidable distributions of size ($P(\sigma)$) and charges ($P(Z)$), which are generally broader for smaller particles. For highly charged particles, short-range repulsions are governed by Coulomb interactions, rather than by intrinsic polyion size, and use of the Gibbs-Bogoliubov inequality linking the free energy of a system of interest to that of suitably chosen reference system, allows a mapping of charge polydispersity onto effective size polydispersity in concentrated colloidal suspensions [7].

In the following we shall address the question: "Do concentrated colloidal suspensions behave as simple liquids", by examining the phase behaviour in section 2, the kinetic glass transition in section 3, the relation between density profiles under gravity and the osmotic equation-of-state in section 4, while section 5 is devoted to highly asymmetric fluid mixtures of hard spheres which may be regarded as a first step towards "non-primitive" models of suspensions which would account for the discrete nature of the suspending fluid.

2. PHASE TRANSITIONS IN CONCENTRATED COLLOIDAL SUSPENSIONS

The ability of natural and synthetic colloids to form crystals, exhibiting iridescence due to Bragg reflection of visible light, has been known and investigated for many years [8]. A brief discussion of crystallization is given below, within the context of the two basic models (hard sphere and Yukawa) introduced in the previous section.

a) Hard spheres, which are the basic model for sterically stabilized colloidal suspensions, have been the object of thorough Statistical Mechanics investigation for several decades. Since there is no energy scale, a monodisperse hard sphere system is entirely characterized by the packing fraction $\eta = \pi\rho\sigma^3/6$, where $\rho = N/V$ is the number of particles per unit volume. Ever since the pioneering work of Alder and Wainwright [9], it is known that hard spheres undergo a strongly first order phase transition from a fluid to a close-packed (FCC or HCP) crystal; careful free energy calculations lead to the estimates $\eta_f = 0.49$ and $\eta_s = 0.54$ for the packing fractions of the coexisting fluid and solid phases [10]. These values are in remarkable agreement with recent observations of quasi monodisperse suspensions of PMMA particles by Pusey and Van Megen [11]. These authors also observed glassy states (characterized by the absence of iridescence) beyond a packing fraction $\eta \simeq 0.60$.

Binary mixtures of hard spheres have been examined, within the framework of the density functional theory of freezing [12], and more recently via extensive Monte Carlo calculations of the free energy [13]. The shape of the fluid-solid phase diagram (where the crystal is assumed to be a substitutional solid solution), changes rapidly with the size ratio $y = \sigma_1/\sigma_2$, turning from spindle shape ($1 > y > 0.94$) to azeotropic ($0.94 > y > 0.87$) and finally to eutectic. Below $y \simeq 0.85$ the miscibility of large spheres in the crystal of small spheres shrinks practically to zero (in agreement with the Hume-Rothery rule for metallic alloys). For smaller size ratios compound formation in well defined proportions of small and large colloidal spheres has been studied experimentally by Yoshimura and Hachisu [8] and by Bartlett and collaborators [2,14].

The case of a polydisperse hard sphere system, with a continuous distribution $P(\sigma)$ of diameters, has also been examined within density functional theory [15]. The main result is that the substitutional crystal becomes thermodynamically, and even mechanically unstable for relative polydispersities $p_\sigma = \left[\overline{(\sigma - \overline{\sigma})^2}\right]^{1/2}/\overline{\sigma}$ exceeding about 15%. A simple argument has been put forward to show that this critical p_σ should be largely independent of the precise shape of the distribution function $P(\sigma)$ [16]. For larger p_σ, glass formation would be kinetically favoured over solid-solid phase separation, in view of the very slow interdiffusion of the various species.

b) The Yukawa model, for charge-stabilized colloidal suspensions (in the absence of Van der Waals interactions), has a richer phase diagram than the hard sphere system. Indeed the "softness" of the repulsion may be tuned by varying the reduced inverse screening length κ in eqn.(2), as would result from a change in the concentration of added salt. When $\kappa \to 0$, the model (augmented by a suitable neutralizing background) reduces to the "one-component plasma" (OCP) which is known to crystallize into a BCC lattice, when the dimensionless Coulomb parameter $\Gamma = U_0/k_BT \equiv Z^2e^2/(ak_BT)$ reaches the value $\Gamma = 178$ [17]. On the other hand for large κ, the potential becomes short-ranged and steeply repulsive, so that freezing into an FCC (or HCP) lattice may be expected. This is indeed confirmed by the anharmonic cell model calculations of Alexander et al. [18] and by the extensive MD simulations of Robbins et al. [19]. The latter predict a BCC-FCC transition in the solid for increasing κ, and a BCC-FCC-fluid triple point located approximately at $\Gamma = U_0/k_BT \simeq 5$ and $\kappa \simeq 6$. Some discrepancies between the theoretical phase diagram for the Yukawa system and recent synchrotron X-ray measurements on charged polystyrene spheres [20] seem to point to an inadequacy of the screened Coulomb model (derived from Poisson-Boltzmann theory) at high concentrations.

As stressed already in the introduction, the screened Coulomb repulsion masks the Van der Waals attractions, thus stabilizing the suspension against flocculation. However in the strong screening regime (i.e. in the presence of a high concentration of added salt) the Coulomb barrier shrinks, thus "uncovering" the Van der Waals attraction between colloidal particles; this leads to a secondary minimum in the DLVO potential. As long as the Coulomb barrier is sufficient to prevent irreversible flocculation due to the singularity

(1) at contact, the secondary minimum may be expected to induce a "liquid-gas"-like phase separation into concentrated (fluid) and dilute (gas) phases of the colloidal particles within the suspending medium whenever the depth ϵ of this potential minimum becomes comparable to k_BT. Careful thermodynamic perturbation calculations show that this is indeed the case, for colloidal particles of minimum size satisfying the constraint:

$$\sigma_{\min}(\mathrm{nm}) = \frac{2.5 \times 10^5}{\Psi_0^2(\mathrm{mV})} \tag{3}$$

where Ψ_0 denotes the electric surface potential of the particles (expressed in milli-Volts) [21]. If the latter has the typical value $\Psi_0 = 25$ mV, $\sigma_{\min} \simeq 400$ nm.

3. BROWNIAN DYNAMICS AND KINETIC GLASS TRANSITION

The previous section emphasized the similarities between the phase behaviour of colloidal suspensions and that commonly observed in atomic materials (e.g. in simple metals and alloys). Recent dynamic light scattering experiments have revealed that concentrated colloidal suspensions may also undergo, upon increasing the concentration, a "kinetic" transition towards a metastable, non-ergodic glassy state, signalled by a non-decaying density autocorrelation function over experimentally accessible time intervals, typically a few seconds ("structural arrest") [22,2].

In this section, we describe results from a Brownian Dynamics simulation of the glass transition in a charge-polydisperse colloidal fluid [23,24]. In particular, we are interested in structural relaxation evolving from the Brownian-motion-like short time dynamics. Within a time step Δt that is small compared to the Brownian time τ_B (i.e. the time a macroion needs to diffuse over a typical interparticle spacing), the displacement of the colloidal particle j is [25]

$$\vec{r}_j(t + \Delta t) = \vec{r}_j(t) + \frac{1}{\xi}\vec{F}_j(t)\Delta t + (\Delta\vec{r})_R + O((\Delta t)^2) \tag{4}$$

where ξ is the solvent friction, taken to be independent of particle configuration, thus neglecting solvent-mediated hydrodynamic interactions. $\vec{F}_j$ is the total force exerted on particle j by the other particles. Moreover, the random displacement $(\Delta\vec{r})_R$ is sampled from a Gaussian distribution of zero mean and variance $6k_BT\Delta t/\xi$. The basic equation (4) for irreversible Brownian Dynamics (BD) should be contrasted with reversible Molecular Dynamics (MD) governed by the short time expansion

$$\vec{r}_j(t + \Delta t) = \vec{r}_j(t) + \vec{v}_j(t)\Delta t + \frac{1}{2m}\vec{F}_j(t)(\Delta t)^2 + O((\Delta t)^3) \tag{5}$$

where $\vec{v}_j$ is the velocity and m the particle mass. This is valid for *atomic* systems and the kinetic glass transition for this kind of dynamics has been

extensively studied by computer simulations [26], experiments [27] and mode coupling theories [28]. However, (5) is not applicable to *colloidal* dynamics due to the presence of solvent friction. In the following, we will compare both kinds of dynamics. Whereas the difference in the short time behaviour between BD and MD is obvious, it turns out that the scenario of the kinetic glass transition is qualitatively different, at least at intermediate times.

In the Yukawa model adopted here, the forces $\vec{F}_j$ are derived from the potential (2) suitably generalized to a charge-polydisperse situation [7]:

$$V_{ij}(r) = U_0 \frac{a}{r} \frac{Z_i Z_j}{\bar{Z}^2} \exp(-\kappa \frac{(r-a)}{a}) \qquad (6).$$

Here U_0 and a set the natural energy and length scale of the colloidal particles and, together with ξ, they define the Brownian time scale $\tau_B = \xi a^2/U_0$. For comparison, the typical time scale for Newtonian dynamics is set by the mass as $\tau_N = (ma^2/U_0)^{1/2}$. The decay parameter κ, due to counterions and added salt, is chosen to be fixed, $\kappa \equiv 7$, for the simulation and the charges Z_i are sampled from a Schultz-distribution [23] with a mean valence $\bar{Z}$ and a relative charge-polydispersity $p_Z = 0.5$. In such strongly polydisperse systems, crystallization is bypassed and formation of an amorphous solid is favoured [15,16]. The density is chosen to be $\rho = a^{-3}$ and the system is slowly cooled from the temperature $T^* \equiv k_B T/U_0 = 0.45$ down to $T^* = 0.10$.

A very clear-cut dynamical diagnostic of the kinetic glass transition is provided by the rapid change in behaviour of the self-part of the Van Hove correlation function

$$G_S(r,t) = \frac{1}{N} < \sum_{j=1}^{N} \delta(\vec{r} - \vec{r}_j(0) + \vec{r}_j(t)) > \qquad (7)$$

The function $P(r,t) = 4\pi r^2 a G_S(r,t)$ shown in Figures 1 and 2 is the probability density for finding a particle at a distance r from its original position after a time t. Above the glass transition, $P(r,t)$ tends rapidly to its hydrodynamic limit governed by the long-time diffusion constant D_L whereas for $T = T_G$ the structure becomes frozen and particles move by thermal activated hopping processes which lead to a build-up of a small secondary peak or shoulder at the mean interparticle spacing a. The hopping processes occur despite the absence of any phonon assistance in BD and can be seen directly by following the trajectories of low-charge particles [23]. Strictly speaking, this crossover is smooth, but it occurs within a very narrow temperature range, and, by this diagnostic, a clearcut estimate of the glass transition temperature $T_G^* \equiv k_B T_G/U_0$ is $0.115 < T_G^* < 0.120$. Correspondingly, the long-time diffusion constant D_L drops to very low values near the glass transition. If the temperature is above and not too close to T_G^*, the data can be well fitted by a power-law $D_L = A(T^* - T_G^*)^\gamma$ with $\gamma \simeq 1.4$. At this point we remark that the behaviour in the MD case is very similar. In particular, the glass transition occurs at the same temperature as in the Brownian case.

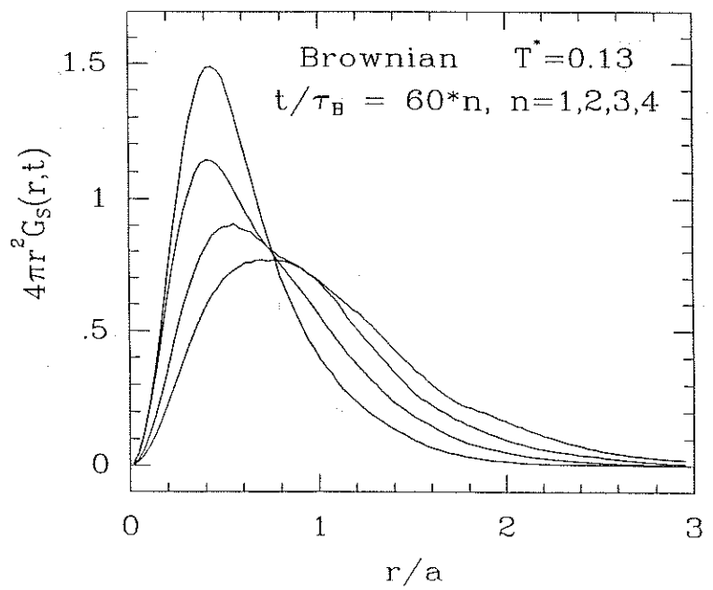

Fig. 1 *The function* $P(r,t) = 4\pi r^2 a G_S(r,t)$ *versus reduced distance* r/a *calculated with Brownian Dynamics; the curves from left to right (or top to bottom) are for increasing time arguments. Results for* $T^* = 0.13$ *and* $t/\tau_B = 60, 120, 180, 240$.

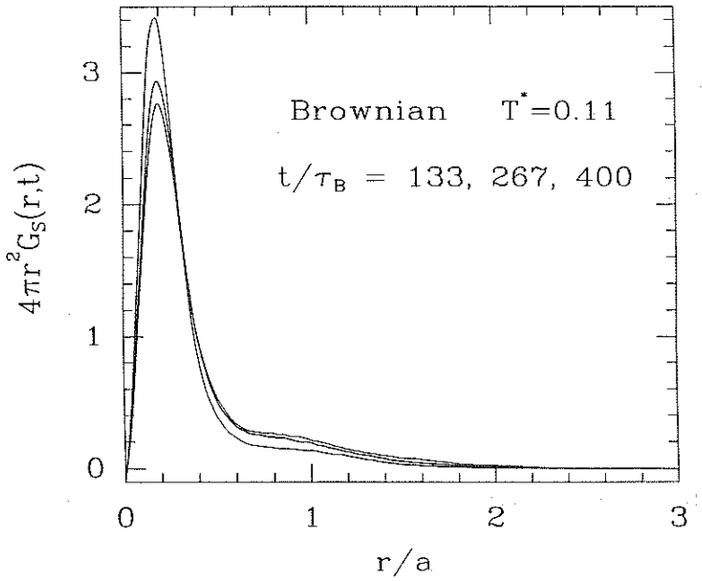

Fig. 2 *Same as Fig. 1 but now for* $T^* = 0.11$ *and* $t/\tau_B = 133, 267, 400$.

Structural relaxation may be conveniently characterized by examining the time-dependence of the density auto-correlation function, or intermediate scattering function for wavevectors k_0 in the vicinity of the main peak of the static structure factor. In this range of wavevectors, this function is close to the spatial Fourier transform $F_S(k_0,t)$ of $G_S(r,t)$. In Figure 3, the relaxation of $F_S(k_0,t)$ is shown on a logarithmic time scale. At the glass transition ($T = T_G$), there is no clear build-up of a plateau nor a clear separation into two different time-scales. The relaxation for large times can tentatively be identified with α-relaxation. Structural arrest occurs only at a temperature well below T_G. This is different from the MD-case, which is illustrated in Figure 4. The underlying glass transition, that occurs at the same temperature as in the BD case, is accompanied by the build-up of a plateau and a separation of time scales. The spectrum $S_S(k_0,\omega)$ of $F_S(k_0,t)$ exhibits a peak at intermediate frequencies, that may be tentatively associated with β-relaxation. For BD, however, this peak is missing. Thus one important conclusion is that β-relaxation is absent for Brownian dynamics.

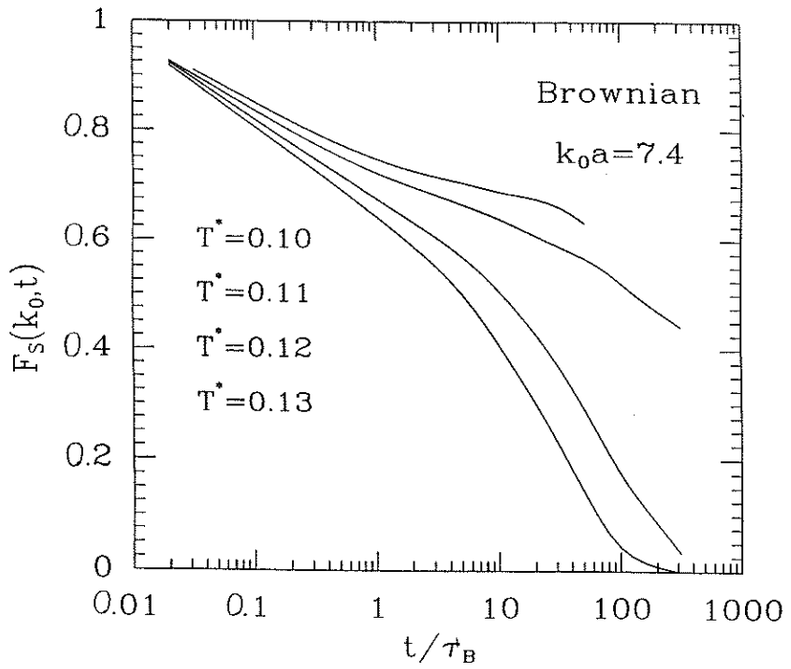

Fig. 3 *$F_S(k,t)$ versus $t^* = t/\tau_B$ on a logarithmic scale for $k = k_0 = 7.4/a$ and (from bottom to top) $T^* = 0.13, 0.12, 0.11, 0.10$ (Brownian Dynamics).*

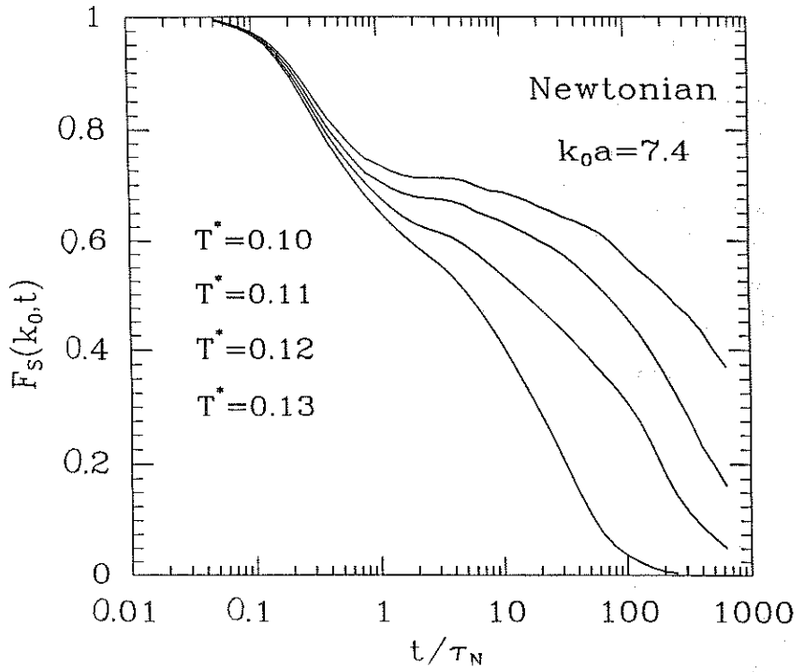

Fig. 4 *$F_S(k,t)$ versus $t^* = t/\tau_N$ on a logarithmic scale for $k = k_0 = 7.4/a$ and (from bottom to top) $T^* = 0.13, 0.12, 0.11, 0.10$ (Newtonian Dynamics).*

The different diffusive behaviour of low-charge and high-charge particles near the kinetic glass transition was studied in detail in Ref. [24]. It was found that the ratio of the corresponding long-time diffusion constants varies considerably near the glass transition. This implies that the high-charge particles "freeze" first and then the low-charge particles follow, but everything happens in a smooth manner as the system is cooled.

4. OSMOTIC PRESSURE FROM DENSITY PROFILES

The equation-of-state of simple atomic or molecular fluids contains much information about the mutual interactions between particles. The variation of the pressure with density and temperature is more sensitive to details of the interactions than, for instance, the pair structure, as measured by X-ray or neutron diffraction. A good illustration of this sensitivity is provided by the semi quantitative information about atomic pair potentials gained from accurate measurements of the second virial coefficient [29]. Similar procedures have not yet been systematically persued in colloidal suspensions, because the osmotic pressure of colloids is generally too weak to be directly measurable. A straightforward application of van 't Hoff's law (valid for non-interacting

particles in suspension) shows that the order of magnitude of the osmotic pressure exerted by sub-micronic particles is typically 1 Pascal or less at room temperature.

However, contrarily to the case of atomic-size particles, the gravitational energy of colloidal particles is easily comparable to the thermal energy k_BT. Hence it is not surprising that the density of suspended particles is highly inhomogeneous under gravity. This observation was first exploited by Perrin [30] who was able to estimate Boltzmann's constant from a measurement of the density profile $\rho(z)$ of dilute suspensions, where interactions between colloidal particles may be neglected, resulting in the familiar exponential density profile (barometric law).

More generally, a careful implementation of the osmotic equilibrium of the suspension shows that the local osmotic pressure $P(z)$ and density $\rho(z)$ are simply related by the hydrostatic equation:

$$\frac{d}{dz}P(z) = -mg\rho(z) \tag{8}$$

where m is the buoyant mass [31] and $P(z) = P(\rho(z))$ under isothermal conditions. In the infinite dilution limit, $P(z) = k_BT\rho(z)$, and Perrin's exponential profile immediately follows. For concentrated suspensions, the profile may be calculated from the knowledge of the equation-of-state $P(\rho)$ of a homogeneous fluid of interacting colloids (local density approximation). Such a calculation can be carried out analytically, leading to a sigmoidally-shaped density profile [31].

Recently, it was suggested that the whole procedure may be inverted, i.e. the osmotic equation-of-state $P(\rho)$ may be extracted from accurate measurements of $\rho(z)$ [32]. Indeed, direct integration of (8) leads to:

$$\beta P(z) = \alpha \int_z^\infty \rho(z')dz' \tag{9}$$

where $\beta = 1/k_BT$ and α is the characteristic inverse gravitational length, $\alpha = \beta mg$, which is typically of the order of a few particle diameters. Elimination of the altitude z between the measured $\rho(z)$ and the resulting $P(z)$ yields directly $P(\rho)$.

This inversion procedure was tested in Ref. [32] by extensive Monte Carlo (MC) calculations of the hard sphere and Yukawa systems subjected to gravity (with $0.1 \lesssim \alpha\sigma \lesssim 1$). Coarse-grained density profiles $\overline{\rho}(z)$ were calculated by convoluting the simulation data for $\rho(z)$ with a resolution function $w(z)$ of width comparable to the particle size, in order to smooth out the oscillations near $z = 0$ due to layering against the hard wall at the bottom of the sample. The local density approximation leading to eqn.(8) applies to the coarse-grained $\overline{\rho}(z)$, and the resulting equation-of-state, obtained by the previously described inversion procedure, agree well with the known homogeneous hard sphere and Yukawa data. These calculations strongly emphasize the sensitivity of the density profiles to the assumed pair interactions. Similar inversions based on true experimental (rather than numerical!) density

profiles would be highly desirable, and could yield useful, although indirect, information about colloidal interactions.

5. TWO FLUID MODEL OF COLLOIDAL SUSPENSIONS

A suspension may be viewed as a "mixture" of two fluids: the "solvent" made up of atomic-size particles (fluid 1), and the fluid of mesoscopic colloidal particles (fluid 2). In view of the very small size ratio $y = \sigma_1/\sigma_2$ (typically $10^{-1} > y > 10^{-4}$), fluid 1 may generally be considered to be a continuum on the length and time scales of the colloidal particles ("primitive" model). As illustrated in section 3, this continuum strongly affects the dynamics of the latter, via Stokesian friction and hydrodynamic interactions, but should have no influence of the static properties of fluid 2. Indeed no account is taken of the suspending fluid in statistical interpretation of the pair structure of the colloidal fluid, as measured by diffraction experiments [2].

In this section we briefly review some recent theoretical results for the simplest "discrete solvent" model of a suspension, namely a highly asymmetric binary mixture of additive hard spheres [33,34,35]. The three partial pair distribution functions $g_{\alpha\beta}(r)$ of this two component system are related to the direct correlation functions $c_{\alpha\beta}(r)$ via the familiar Ornstein-Zernike (OZ) relations [3]:

$$h_{\alpha\beta}(r) \equiv g_{\alpha\beta}(r) - 1 = c_{\alpha\beta}(r) + \rho \sum_\gamma x_\gamma c_{\alpha\gamma} * h_{\gamma\beta}(r) \tag{10}$$

where x_γ denotes the number concentration of species γ $(1 \leq \alpha, \beta, \gamma \leq 2)$ and ρ is the total number density, while $*$ denotes a convolution product. The OZ relations (8) must be supplemented by a closure relation; for hard sphere systems the most common relation is the Percus Yevick (PY) closure:

$$g_{\alpha\beta}(r) = \Theta(r - \sigma_{\alpha\beta})[1 + \gamma_{\alpha\beta}(r)] \tag{11}$$

where Θ denotes the Heavyside step-function, and $\gamma_{\alpha\beta} = h_{\alpha\beta} - c_{\alpha\beta}$. The set of eqns.(10)-(11) has been solved analytically [36] and leads to the prediction of complete miscibility of fluid hard sphere mixtures, irrespective of the size ratio $y = \sigma_1/\sigma_2$ [37]. However, upon closer inspection, it may be shown that the contact value of the pair distribution of large spheres, $g_{22}^{PY}(r = \sigma_2^+)$ diverges as $1/y$ when the size ratio goes to zero [34,35]. This effective "stickiness" of large spheres is a manifestation of the "osmotic depletion" phenomenon predicted earlier for dispersions of spherical colloids and non-adsorbing polymer coils, modeled by interpenetrating spheres [38,39]. The osmotic depletion effect is known to drive phase separation, which is not surprising in view of the non-additivity of colloid and polymer diameters [40]. Despite the prediction of complete miscibility by the PY theory for hard sphere mixtures with additive diameters, it is not unreasonable to explore the possibility of phase separation on the basis of more accurate integral equations.

PY theory is known to exhibit thermodynamic inconsistency, as illustrated by the significant differences of the equations-of-state derived from the virial or compressibility relations [3]. This inconsistency may be overcome by the use of thermodynamically self-consistent closures, among which one of the most successful is that due to Rogers and Young (RY) [41], which reads for hard spheres:

$$g_{\alpha\beta}(r) = \Theta(r-\sigma_{\alpha\beta})\Big\{1+\frac{\exp[\gamma_{\alpha\beta}(r)f_{\alpha\beta}(r)]-1}{f_{\alpha\beta}(r)}\Big\} \qquad (12)$$

where the switching functions $f_{\alpha\beta}(r)$ are conveniently chosen to be of the form $1-\exp(\xi_{\alpha\beta}r)$, with $\xi_{\alpha\beta}$ assumed to be of the simple scaling form $\xi_{\alpha\beta}=\xi/\sigma_{\alpha\beta}$. The single dimensionless parameter ξ is varied until the virial and compressibility estimates of the equation-of-state coincide.

We have solved the RY equations numerically, for many values of the two partial packing fractions $\eta_\alpha=\pi\rho x_\alpha\sigma_\alpha^3/6$, and for several size ratios y [35]. The calculated pressure agrees surprisingly well, for all cases that were considered, with the semi-empirical equation-of-state of Mansoori et al. [42]. Spinodal instability of the mixture is signalled by the divergence of the long wavelength limit of the concentration-concentration structure factor [3]:

$$\lim_{k\to 0} S_{cc}(k) = \frac{Nk_BT}{(\partial^2 G/\partial x_1^2)_{N,P,T}} \qquad (13)$$

In figure 5 we show constant reduced pressure ($P^*=P\sigma_1^3/k_BT$) plots of $\Lambda = x_1x_2/S_{cc}(0)$, as obtained from the numerical solutions of the RY equations, versus $x_2^{1/3}$, for the size ratio $y=0.1$. At low pressures, ($P^*\lesssim 0.05$), there is complete miscibility for all concentrations x_2. At higher pressures ($P^*>0.1$), Λ drops to zero as x_2 is increased, so that the corresponding hard sphere mixtures are thermodynamically unstable. Thus we predict a phase separation of highly asymmetric hard sphere mixtures, beyond a pressure-dependent concentration of large (colloidal) spheres immersed in the discrete suspending medium of small spheres. The critical pressure P_c^* above which phase separation occurs is in the range $0.1\gtrsim P_c^*\gtrsim 0.05$. The conjugate phase may be either another fluid phase (richer in large spheres), or one or several solid phases of different compositions. In the former case, there exists a fluid-fluid-solid triple point at a reduced pressure P^* above P_c^*, while in the latter the second fluid phase (rich in large spheres) is pre-empted by crystallization.

The behaviour of Λ as a function of $x_2^{1/3}$ is somewhat unusual for $P^*=0.07$, where Λ goes negative twice as x_2 increases. The first "loop" is compatible with fluid-fluid coexistence, but the second "loop" occurs at very high packing fractions η_2 of the large spheres, suggesting that this second phase separation is in fact pre-empted by cristallization. Integral equations, based on the explicit assumption of translational invariance, are of course uncapable of accounting for fluid-solid coexistence.

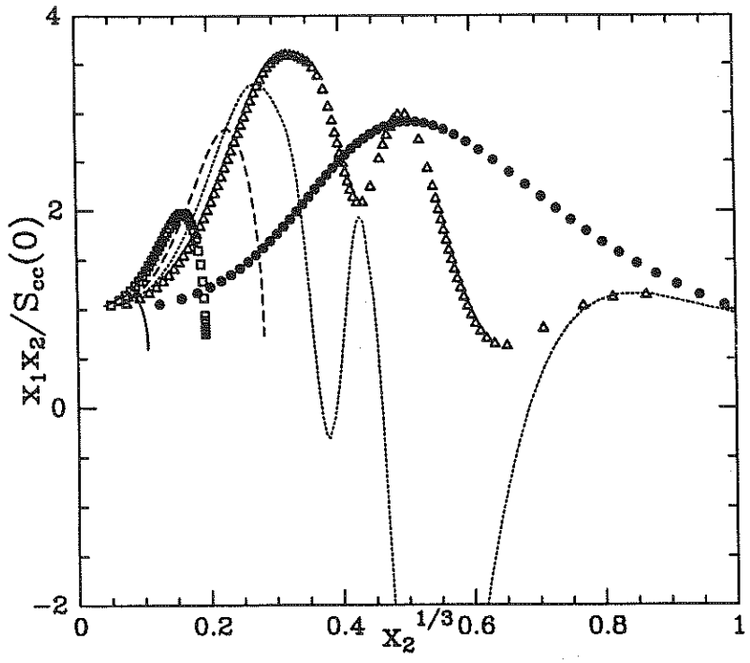

Fig. 5 *Ratio* $x_1x_2/S_{cc}(0)$ *versus* $x_2^{1/3}$ *for a size ratio* $y=0.1$ *and for* $P^*=0.5$ *(full curve),* 0.2 *(squares),* 0.1 *(dashed curve),* 0.07 *(dots),* 0.05 *(triangles) and* 0.01 *(circles).*

Although a complete phase diagram for highly asymmetric hard sphere mixtures cannot be drawn yet, it is clear that the RY results strongly suggest a lack of miscibility of the small and large spheres in the fluid phase.

ACKNOWLEDGMENTS

The authors gratefully acknowledge the crucially important collaboration of J.L. Barrat and J.N. Roux for several parts of the work presented here. Some points concerning sections 4 and 5 were clarified after stimulating discussions with H.N.W. Lekkerkerker.

REFERENCES

1. E.J.W. Vervey and J.Th.G. Overbeek, "Theory of Stability of Lyophobic Colloids" (Elsevier, Amsterdam 1948)
2. For an excellent recent review on experimental and theoretical aspect of colloidal suspensions see P.N. Pusey, in "Liquids, Freezing and the Glass Transition", edited by J.P. Hansen, D. Levesque and J. Zinn-Justin (North Holland, Amsterdam,1991).
3. J.P. Hansen and I.R. Mc Donald, "Theory of Simple Liquids", 2^{nd} edition (Academic Press, London, 1986)
4. L. Belloni, J. Chem. Phys. **85**, 519 (1986).
5. H. Löwen, P. Madden and J.P. Hansen, to be published.
6. R. Car and M. Parrinello, Phys Rev. Letters **55**, 3471 (1985).
7. H. Löwen, J.N. Roux and J.P. Hansen, J. Phys. Cond. Matt. **3**, 997 (1991).
8. For reviews, see P. Pieranski, Contemp. Phys. **24**, 25 (1983), and the proceedings of the "Winter Workshop on Colloidal Crystals", edited by P. Pieranski and F. Rothen, J. Phys. Colloq. **46**, C3 (1985).
9. B.J. Alder and T.E. Wainwright, J. Chem. Phys. **27**, 1208 (1957).
10. W.G. Hoover and F. Ree, J. Chem. Phys. **49**, 3609 (1968).
11. P.N. Pusey and W. Van Megen, Nature **320**, 340 (1986).
12. J.L. Barrat, M. Baus and J.P. Hansen, J. Phys. C **20**, 1413 (1987).
13. W.G.T. Kranendonk and D. Frenkel, Mol. Phys. **72**, 679 and 699 (1991).
14. see the poster presented by P. Bartlett at this NATO ASI.
15. J.L. Barrat and J.P. Hansen, J. Phys. **47**, 1547 (1986).
16. P.N. Pusey, J. Phys. **48**, 709 (1987).
17. E.L. Pollock and J.P. Hansen, Phys. Rev. A **8**, 3110 (1973).
18. D.S. Hone, S. Alexander, P.M. Chaikin and P. Pincus, J. Chem. Phys. **79**, 1474 (1983).
19. M.O. Robbins, K. Kremer and G.S. Grest, J. Chem. Phys. **88**, 3286 (1988).
20. E.B. Sirota, H.D. Ou-Yang, S.K. Sinha, P.M. Chaikin, J.D. Axe and Y. Fuji, Phys. Rev. Letters **62**, 1524 (1989).
21. J.M. Victor and J.P. Hansen, Trans. Faraday Soc. II **81**, 43 (1985).
22. P.N. Pusey and W. van Megen, Phys.Rev.Lett. **59**, 2083 (1987); Ber. Bunsenges. Phys. Chem. **94**, 225 (1990); Phys. Rev. A **43**, 5429 (1991);
23. H. Löwen, J.P. Hansen, J.N. Roux, Phys. Rev. A (in press).
24. H. Löwen, J.P. Hansen, in: "Recent Developments in the Physics of Liquids", Symposium in Honor to P. A. Egelstaff, IOP Publishing, Bristol, 1991.
25. D.L. Ermak, J.Chem.Phys. **62**, 4189, 4197 (1975).

26. see e.g. the review of J. L. Barrat, M. Klein, Ann. Review Phys. Chem. **42**, 23 (1991).
27. F. Mezei, W. Knaak and B. Farago, Phys. Rev. Lett. **58**, 571 (1987); W. Knaak, F. Mezei and B. Farago, Europhys. Lett. **7**, 529 (1988).
28. For a recent review, see W. Götze, in "Liquids, Freezing and the Glass Transition", edited by J.P. Hansen, D. Levesque and J. Zinn-Justin (North Holland, Amsterdam,1991).
29. J.O. Hirschfelder, C.F. Curtiss and R.B. Bird, " Molecular Theory of Gases and Liquids" (John Wiley, New York, 1954).
30. J. Perrin, J. Phys. série 4 **9** 5, (1910).
31. A. Vrij, J. Chem. Phys. **72**, 3735 (1991).
32. J.L. Barrat, T. Biben and J.P. Hansen, to be published (1991).
33. D. Henderson, J. Colloid Interface Sci. **121**, 486 (1988).
34. T. Biben and J.P. Hansen, Europhys. Lett. **12**, 347 (1990).
35. T. Biben and J.P. Hansen, Phys. Rev. Lett. **66**, 2215 (1991); and J. Phys. Cond. Matt. (in press).
36. J.L. Lebowitz, Phys. Rev. A **133**, 895 (1964).
37. J.L. Lebowitz and J.S. Rowlinson, J. Chem. Phys. **41**, 133 (1964).
38. S. Asakura and F. Oosawa, J.Polymer Sci. **23**, 183 (1958).
39. A. Vrij, Pure and Appl.Chem. **48**, 471 (1976).
40. H.N.W. Lekkerkerker, Coll. and Surf. **51**, 419 (1990).
41. F.J. Rogers and D.A. Young, Phys.Rev. A **30**, 999 (1984).
42. G.A. Mansoori, N.F. Carnahan, K.E Starling and T.W. Leland, J. Chem. Phys. **54**, 1523 (1971).